Dispatch Scheduling for a Wind Farm With Hybrid Energy Storage Based on Wind and LMP Forecasting

Meng Liu, *Student Member, IEEE*, Franklin L. Quilumba, *Member, IEEE*, and Wei-Jen Lee, *Fellow, IEEE*

***Abstract*—In a deregulated power market, the real-time wholesale market price of electricity varies dramatically within a single day due to the availability of the resources. Moreover, the price of electricity can be different from one location to the other at the same time period due to the location of the available resources and transmission constraints. This is the so-called locational marginal price (LMP). Since wind power is noncontrollable and partially unpredictable, it is difficult to schedule its output to exploit LMP variations. While energy storage system (ESS) may accommodate wind farm output, it requires significant initial financial commitment. Accurately forecasted wind power and LMP information can reduce the required capacity and make it financially feasible for the ESS to perform desired functions. In this paper, artificial neural network (ANN) technique is employed to forecast the day-ahead wind power and LMP, and a hybrid ESS consisting of two storage facilities is developed. The primary ESS is utilized for the optimizing wind-storage system production schedule with day-ahead forecasting data, while the secondary ESS is applied to address the forecasting errors during real-time operation. With this hybrid ESS design, financial benefits are achieved for the wind farm.**

***Index Terms*—Hybrid energy storage systems, locational marginal price (LMP) forecasting, renewable energy, wind power dispatch schedule, wind power forecasting.**

NOMENCLATURE

ANN	Artificial neural network.
C_p	Cost of pump system.
E_B	Available battery capacity.
$E_B^{\max}$	Maximum available battery capacity.
E_R	Available water reservoir energy.
$E_R^{\max}$	Maximum available water reservoir energy.
ERCOT	Electric Reliability Council of Texas.
ESS	Energy storage system.
LMP	Locational marginal price.
LMP_{thr}	LMP threshold for secondary ESS operation.
P	Power delivered to the grid based on forecasting.
P^{act}	Actual power delivered to the grid.
PHS	Pumped hydroelectric storage.
P_d	Power dissipated by dump load.
P_h	Power generated by hydro unit.
$P_h^{\max}$	Maximum hydro unit power generation.
$P_h^{\min}$	Minimum hydro unit power generation.
P_g	Forecasted total available wind power.
P_g^{act}	Actual total available wind power.
P_{mis}	Actual and forecasted wind power mismatch.
P_p	Power consumed by pump system.
$P_p^{\max}$	Maximum pump system power consumption.
$P_p^{\min}$	Minimum pump system power consumption.
P_w	Wind power directly delivered to the grid.
P_{ch}	Battery charge power.
P_{dch}	Battery discharge power.
η_{bch}	Battery charge efficiency.
η_{bdch}	Battery discharge efficiency.
η_h	Hydro unit efficiency.
η_p	Pump system efficiency.

Manuscript received June 25, 2014; revised October 12, 2014; accepted November 12, 2014. Date of publication November 20, 2014; date of current version May 15, 2015. Paper 2014-ESC-0250.R1, presented at the 2014 IEEE Industry Applications Society Annual Meeting, Vancouver, BC, Canada, October 5–9, and approved for publication in the IEEE TRANSACTIONS ON INDUSTRY APPLICATIONS by the Energy Systems Committee of the IEEE Industry Applications Society. This paper is based upon work supported by the National Science Foundation under Grant EFRI-1038234.

M. Liu and W.-J. Lee are with the Energy Systems Research Center, The University of Texas at Arlington, Arlington, TX 76019 USA (e-mail: meng.liu@mavs.uta.edu; wlee@uta.edu).

F. L. Quilumba is with the Electrical Energy Department, National Polytechnic School, Quito EC170102, Ecuador (e-mail: quigufrale@ieee.org).

Digital Object Identifier 10.1109/TIA.2014.2372043

I. INTRODUCTION

WIND POWER, as a promising renewable energy resource for supporting continuously growing electricity demand, bears the disadvantages of noncontrollable variability and partial unpredictability, which present challenges for large-scale integration into the power system [1]. To maintain stable system frequency, the mechanical energy driving the generators should balance the electrical energy consumed by loads and losses at all times. ESSs may work as a solution to shape the variable wind generation to follow certain production plans, which benefits both system operation and market participation [2]. However, it requires significant financial commitment for a large-scale ESS. Accurately forecasted wind power and LMP information can reduce the required capacity and make it financially feasible for the ESS to perform desired functions. This paper focuses on the operation of the wind farm with appropriate ESS installation to realize the financial benefits of the wind farm and balance the supply and demand of the system.

Wind power forecasting methods can generally be classified into two groups: physical methods and statistical methods [3]–[5]. Physical methods employ meteorological data and physical laws to forecast the wind speeds and directions and feed the results into wind turbine power curves to calculate the corresponding power outputs [6]. Statistical methods attempt to develop models using historical wind power data [7]. Hybrid methods that combine both ideas are also proposed to improve forecasting accuracy [8], [9]. Various algorithms have been proposed to develop wind forecasting models, including

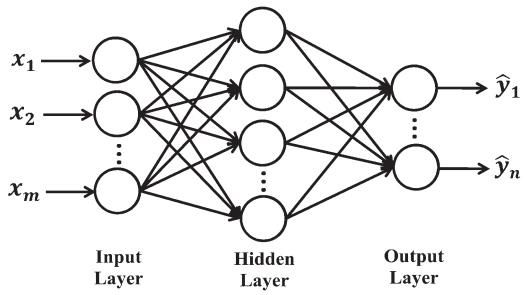

Fig. 1. Structure of three-layer feedforward ANN model.

autoregressive models [10], [11], ANN [12], [13], support vector machines [14], [15], fuzzy logic [16], [17], etc.

On the other side, LMP forecasting in competitive electricity markets is critical for any decision-making process of market participants. Different candidates may impact LMP, including the system load profile, fuel price, transmission congestion, and generation facility behaviors [18]. LMP carries a nonlinear relationship with historical values and the forecasted values of the influencing factors [19]. ANN [20]–[22] techniques are one of the most commonly used methods for LMP forecasting.

With day-ahead wind power and LMP forecasting results, a wind farm with ESS is able to optimize its operation schedule to obtain maximum financial benefits. Research works have been done to optimize wind farm and ESS operations by forecasting wind power and designing operation strategies accordingly [2], [23]. However, the gap between the predicted and the actual wind power is rarely considered.

In this paper, the day-ahead wind power and LMP information are forecasted by ANN, and the forecasting results are used to dispatch the primary ESS to store wind power when the LMP is low and deliver electricity during peak hours when the LMP is high. Due to the required response speed, the mismatch between the forecasted wind power and actual wind power is adjusted by a second set of ESS in real-time operation to enhance the performance.

The remainder of this paper is organized as follows. Section II introduces the technique of ANN and its applications for wind power and LMP forecasting. Section III describes the technology selection of the hybrid ESS. Section IV presents the day-ahead optimization of the wind farm and the primary ESS. In Section V, the secondary ESS is utilized to improve real-time operation. Section VI analyzes the results of two study cases. Section VII draws conclusions.

II. ANN-Based Wind Power and LMP Forecasting

ANNs are massively parallel distributed processors consisting of simple computing units, called neurons, to mimic the learning processes that the brain performs by constructing input–output mapping of the given examples [13], [24]. The complex nonlinear relationship between input and output variables can be used to make future predictions.

The general structure of three-layer feedforward ANNs which are composed of an input layer, a hidden layer, and an output layer is shown in Fig. 1. It has been stated that, as long as enough neurons are chosen, one hidden layer is enough to estimate any continuous function for applications [13], [25]. This paper utilizes forward heuristic simulation to decide the proper number of hidden units. The training process starts with a small number of hidden units and increases the unit number by one until no significant improvement is achieved to avoid overfitting issues.

The selection of input variables is problem dependent; both influencing factors and historical data may affect the accuracy of the forecasting results. The forecast performances are evaluated by the mean absolute percentage error (MAPE) defined in (1), which is the ratio between absolute forecast errors and the actual values

$$MAPE = \frac{1}{M}\sum_{i=1}^{M}\left|\frac{y_i - \hat{y}_i}{y_i}\right| \times 100\% \tag{1}$$

where

M total number of data points;
y_i ith actual value;
$\hat{y}_i$ ith forecasted value.

The process of wind power and that of LMP forecasting are discussed respectively in the following sections.

A. Wind Power Forecasting

The hybrid forecasting method is adopted in this study where both numerical weather prediction (NWP) data and historical wind farm power outputs are used to predict the wind power for the next day in 15-min time steps. The available data are the 9-month power output of a wind farm in west Texas, with a total installation capacity of 160 MW. The weather information of the weather station located in the wind farm of the same year can be accessed from [26] and used as NWP data. Based on the correlation coefficient analysis defined in (2), time indices (hour, quarter) and several meteorological data are used as ANN inputs, including temperature, pressure, sine and cosine for wind direction, wind speed, and humidity of the forecasting day

$$\rho_{x,y} = \frac{Cov(X,Y)}{\sigma_x \sigma_y} = \frac{\sum(x-\mu_x)(x-\mu_y)}{\sqrt{\sum(x-\mu_x)^2 \sum(y-\mu_y)^2}} \tag{2}$$

where

$\rho_{x,y}$ correlation coefficient between X and Y;
σ_x, σ_y standard deviation of X and Y;
μ_x, μ_y mean of x and y.

The autocorrelation function defined in (3) is applied for selecting the appropriate lagged values for the power output data. The last 6 h of day-ahead power outputs in 15-min time steps is chosen as inputs

$$r_k = \frac{\sum_{t=k+1}^{T}(y_t - \mu_y)(y_{t-k} - \mu_y)}{\sum_{t=1}^{T}(y_t - \mu_y)^2} \tag{3}$$

where

r_k autocorrelation coefficient between y_t and y_{t-k};
T length of time series;
μ_y mean of y.

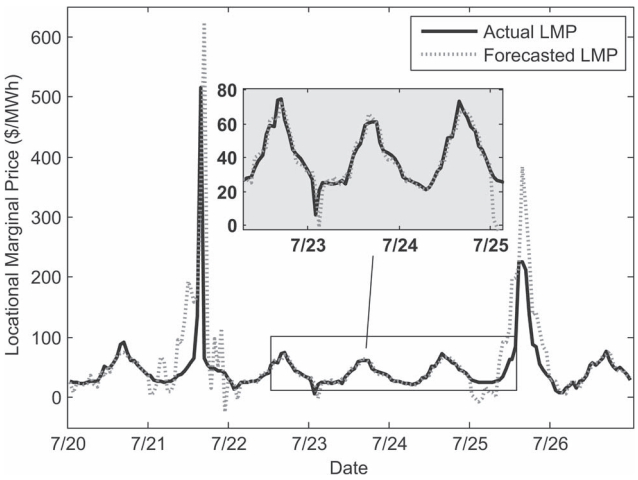

Fig. 2. Actual and the forecasted hourly LMP of a sample week in July.

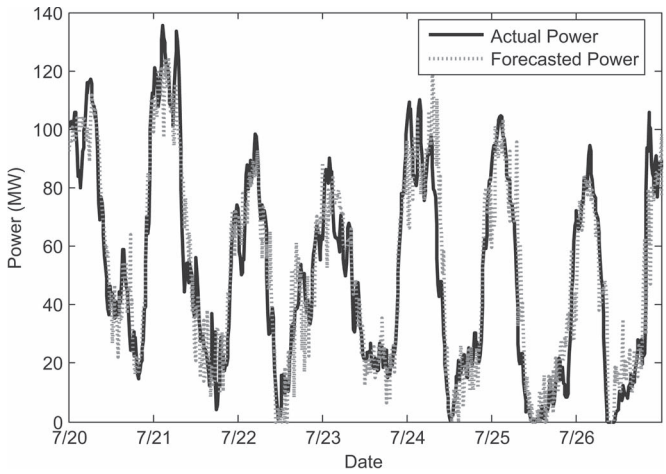

Fig. 3. Actual and the forecasted 15-min wind power of a sample week in July.

Therefore, the networks shown in Fig. 1 is composed of three layers for wind power forecasting, while the input layer has 32 neurons, the output layer has 1 neuron (power output), and the hidden layer is calculated to have 20 neurons. The hyperbolic tangent activation function is employed with the networks, and the Levenberg–Marquardt method is used to train the model. The data from January to June are used to train the network, and the data from July to September are used for testing. The MAPE of the model is calculated to be 10.24%. The actual and the forecasted wind power of a week in July is plotted in Fig. 2 as an example. The results of the ANN forecasting is accurate enough to forecast the day-ahead wind power, and the results will be used for day-ahead wind and hybrid ESS system operation optimization in Section IV.

B. LMP Forecasting

In the nodal market, LMP is the cost to provide the last megawatt of power at a given node; it includes the marginal generation cost, marginal loss cost, and marginal transmission congestion cost [27]. In the ERCOT, wind generation is not required to submit offers in the day-ahead market like other qualified scheduling entities (QSEs). Wind generation resources are allowed to generate according to the wind condition, and it usually participates in the real-time market as a price taker [28], [29]. Thus, the day-ahead LMP forecasting provides essential information for optimizing the wind-hybrid ESS dispatch schedule. Since LMP does not fluctuate as frequently as wind power output, the time step of LMP forecasting is chosen at 1 h.

ANN technique is applied for the day-ahead hourly LMP forecasting in this paper. The hourly LMP and load profile of the ERCOT real-time market are used for the study. Based on the correlation coefficient and autocorrelation coefficient analysis discussed in Section II-A, the variables feeding the input layer are as follows: day of the week, hour, whether holiday, forecasted temperature, system load, and the lagged values of LMP_{t-k}, corresponding to the indices $k = 24$, 25, 26, 48, 49, 50, 72, 73, 74, 96, 97, 98, 120, 121, 122, 144, 145, and 146. For LMP forecasting, the input layer has 23 neurons, the hidden layer is calculated to have 18 neurons, and the only output neuron is LMP.

The annually 15-min LMP data from ERCOT are available, and the hourly LMP data feeding into the ANN are the average value of each hour at the node nearest to the wind farm. The data from January to June are used to train the network, and the data from July to September are used for testing. The actual and the forecasted hourly LMP of the same sample week as wind power are plotted in Fig. 3. The MAPE is calculated to be 17.38%. The majority of the forecasting errors come from the price spikes.

Two price spikes can be observed in the weekly LMP curve in Fig. 3. The price spikes are possibly caused by either transmission congestions or deficiency of generation resources. From Fig. 3, LMP forecasting for an operation day without a price spike can reflect the price variations more accurately, as shown by the magnifying window. However, when LMP spikes happen, such as in July 21 and July 25, the mismatches between the actual and the forecasted LMP become quite large.

It can be observed from Figs. 2 and 3 that the wind farm has higher output in the early morning and at late night while the LMP has higher values, even spikes, during the peak hours, typically in the afternoon. Therefore, the application of hybrid ESS can optimize the production plan of the wind-storage system according to LMP variations to realize financial benefits from the power markets.

III. Hybrid ESS Technology Selection

The hybrid ESS is composed of two sets of ESS in this study. The primary ESS is utilized for optimizing wind-storage system production with day-ahead forecasting data. Different types of technologies have been adopted for bulk energy storage in power system, while several studies suggest that pump hydroelectric storage (PHS) is the most widely used large-scale ESS because of technology maturity, large storage capacity, long storage period, high round-trip efficiency, and relatively low capital cost per unit energy [2], [30], [31]. Therefore, PHS is chosen as the primary ESS in this study, where the pump will elevate the water to an upper reservoir during off-peak hours and a turbine will generate electricity when the water is released during peak hours.

In real-time operation, the forecasting errors are addressed by a secondary ESS. With a smaller operation time step (15 min is

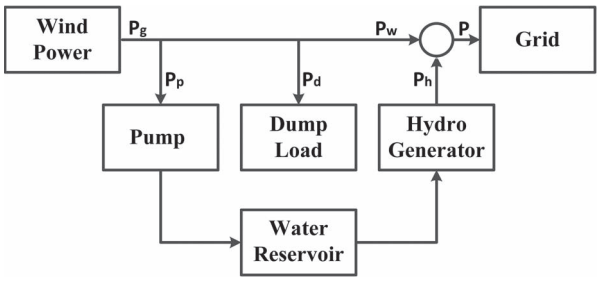

Fig. 4. Day-ahead operation of wind farm and the primary ESS.

chosen), the secondary ESS reacts to the actual wind power and LMP data and adjusts the total production schedule accordingly.

Compared with the primary ESS, the secondary ESS requires smaller installation capacity and faster response time. Being highly modular and having low standby losses, rechargeable batteries can respond very rapidly to smooth out load changes and cogenerated power. Various rechargeable batteries are available nowadays, among which the sodium sulfur (NaS) battery is preferred in this study due to its very high electrical efficiency, long cycle life, and potential low cost [30].

IV. Day-Ahead Wind-ESS Optimization

For wind-ESS operation optimization with day-ahead wind power and LMP forecasting data, the available wind power can be delivered to the grid directly, stored to the primary/secondary ESS and redelivered to the grid later, or dissipated by the dump load (or by wind power curtailment), as shown in Fig. 4.

To decrease the wear and tear costs of hydro units, the dispatch is scheduled for each hour. The daily operation optimization function is defined as

$$\max_{P^{(i)},P_p^{(i)}} \sum_{i=1}^{24} \left(P^{(i)} \times LMP^{(i)} - P_p^{(i)} \times C_p \right) \tag{4}$$

where the objective is to maximize the total daily revenue; (i) is the number of time interval. The revenue is calculated from the sale of wind power in different hour at different LMP subtracting the cost of operating the pump system.

The optimization is subject to the following constraints.

1) Power Balance Constraints:

$$P^{(i)} = P_w^{(i)} + P_h^{(i)} \tag{5}$$

$$P_g^{(i)} = P_w^{(i)} + P_p^{(i)} + P_d^{(i)}. \tag{6}$$

2) Delivered Wind Power Constraints:

$$P_w^{(i)} \geq 0.$$

3) Dump Load Constraints:

$$P_d^{(i)} \geq 0. \tag{8}$$

4) Pump Output Constraints:

$$P_p^{\min} \leq P_p^{(i)} \leq P_p^{\max}. \tag{9}$$

5) Hydro Unit Output Constraints:

$$P_h^{\min} \leq P_h^{(i)} \leq \min\left(P_h^{\max}, \eta_h \frac{E_R^{(i)}}{1h} \right). \tag{10}$$

The output of the hydro unit is limited by its own power limits and the available energy stored in the upper water reservoir.

6) Water Reservoir Energy Constraints:

$$E_R^{(i+1)} = E_R^{(i)} + \left(\eta_p P_p^{(i)} \times (1h) - \frac{P_h^{(i)}}{\eta_h \times (1h)} \right) \tag{11}$$

$$0 \leq E_R^{(i)} \leq E_R^{\max} \tag{12}$$

$$E_R^{(1)} = E_R^{(24)} = E_R^{\max} \times k. \tag{13}$$

This constraint limits that the power consumed by the pump system can only be supplied by the wind farm.

The energy stored in the water reservoir at the beginning of each hour is determined by the initial energy of the previous hour and the output of both pump system and hydro generation units during the previous hour. To make the operation strategy available for longer time span, the initial and final energy levels of an operation day are predefined by an energy level factor k as shown in (13).

V. Real-Time Wind-ESS Dispatch

In real-time operation, the primary ESS system is dispatched based on the optimal schedule developed from day-ahead forecasting information. While the actual wind power output may differ from the forecasted value, the secondary ESS either compensates the power mismatches or exploits the excess wind power concerning its energy and power limits. In the real-time power market, ERCOT publishes the settlement price for each node 5 min ahead of the operation time. The prices at 0, 15, 30, and 45 min of each hour are used as actual LMP and are used for price comparison for the next 15 min. The actual LMP is compared with a threshold price $(LMP_{\rm thr})$, which is determined according to LMP forecasting to reduce unnecessary or uneconomic battery cycling. The algorithm of dispatching the secondary ESS is shown in Algorithm 1.

Algorithm 1 Secondary ESS dispatch

For each time interval (i)
  if $P_g^{\rm act(i)} > P_g^{(i)}$ ($P_{\rm mis}$ is positive)
    if $LMP^{(i)} < LMP_{\rm thr}$
      (*charge battery until* $E_B^{\max}$; *deliver rest power to grid*)
      $P_{\rm ch}^{(i)} = \min[P_{\rm ch}^{\max}, P_{\rm mis}, \eta_{bch} \cdot (E_B^{\max} - E_B^{(i)})/t]$
      $P^{\rm act(i)} = P^{(i)} + P_{\rm mis}$
      $E_B^{(i+1)} = E_B^{(i)} + P_{ch}^{(i)} \times t$
    else $(LMP^{(i)} > LMP_{\rm thr})$
      (*deliver wind power and battery energy to grid*)
      $P_{\rm dch}^{(i)} = \min[P_{\rm dch}^{\max}, \eta_{\rm bdch} \cdot (E_B^{(i)} - E_B^{\min})/t]$
      $P^{\rm act(i)} = P^{(i)} + P_{\rm mis} + P_{\rm dch}^{(i)}$
      $E_B^{(i+1)} = E_B^{(i)} - P_{\rm dch}^{(i)} \times t$
    end if
  else $(P_g^{\rm act(i)} < P_g^{(i)}, P_{\rm mis}$ is negative)
    if $LMP^{(i)} < LMP$thr
      (*deliver less wind power to grid; charge reservoir*)
      $P^{\rm act(i)} = P^{(i)} + P_{\rm mis}$
      $E_B^{(i+1)} = E_B^{(i)}$

else $(LMP^{(i)} > LMP_{\rm thr})$
(*discharge battery; deliver energy to grid*)
$P_{\rm dch}^{(i)} = \min[P_{\rm dch}^{\max}, \eta_{\rm bdch} \cdot (E_B^{(i)} - E_B^{\min})/t]$
$P^{\rm act(i)} = P^{(i)} + P_{\rm dch}^{(i)} + P_{\rm mis}$
$E_B^{(i+1)} = E_B^{(i)} - P_{\rm dch}^{(i)} \times t$
$E_R^{(i+1)} = E_R^{(i+1)} + \eta_p P_{\rm mis}$
end if
end if

In each 15-min time interval, when the actual wind power exceeds the forecasted value, real-time LMP will be compared with $LMP_{\rm thr}$ to determine the strategy to use the surplus wind power. The secondary ESS will be charged until its maximum capacity when the LMP is lower than $LMP_{\rm thr}$ to shift the power to peak hours; when LMP exceeds $LMP_{\rm thr}$, the extra wind power will be directly delivered to the grid to gain financial benefits.

On the contrary, when the actual wind power is lower than the forecasted level, if real-time LMP is less than $LMP_{\rm thr}$, instead of being delivered to the grid, wind power is either consumed by the pump system to elevate water to the upper reservoir or offset by the reduction of the generation of the PHS; if real-time LMP is greater than $LMP_{\rm thr}$, the energy stored in the secondary ESS will be discharged and sent to the grid to take advantage of the high LMP. At the same time, the output of the primary ESS will be used to accommodate possible deficits of the wind power.

VI. Application Results and Discussion

Numerical simulation results of sample cases are used to illustrate the benefits of the proposed dispatch method.

A. Assumptions and Parameter Selection

ESS can contribute to grid reliability needs, defer transmission, and distribution upgrade investments as well as integrate renewable generation resources. The advantages of implementing ESS have been realized in recent years, and the installation of ESS starts to become mandatory. For example, in October 2013, the California Public Utilities Commission sets an energy storage goal for utilities of installing 1.3-GW batteries by 2020 [32]. Since the main goal of this paper is to design the operation strategy of the wind farm with hybrid ESS, the installation and maintenance costs of the ESS are not considered in the calculation.

The total available primary storage capacity is defined as 80% of the 2-h wind farm installation capacity, which is 256 MWh. The efficiency of the pump system and that of the hydro unit are both set at 87%, with a round-trip efficiency $\eta_r = \eta_p \times \eta_h = 75.7\%$. The power output limits of the hydro units are defined as 10 and 50 MW for the minimum and maximum, respectively, and the pump system can consume from 0 to 50 MW. The operation cost of the pump system is set as \$2/MWh. The energy level factor k of the primary ESS is set as 50%.

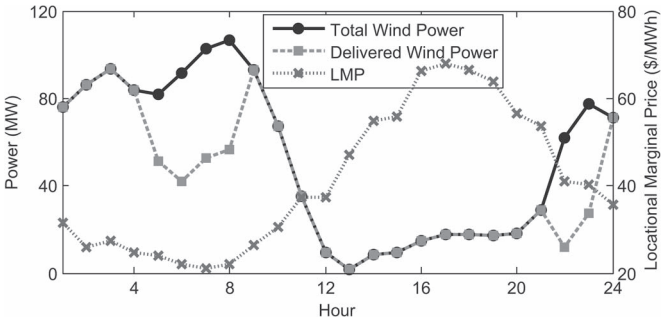

Fig. 5. Total wind power, delivered wind power (left axis), and LMP (without price spikes, right axis) for July 24.

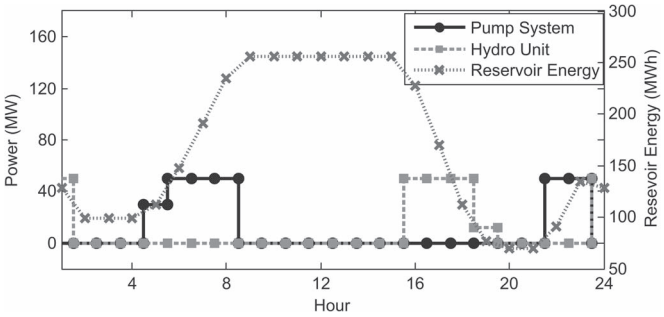

Fig. 6. Pump system consumption, hydro unit output (left axis), and water reservoir energy level (right axis) for July 24.

For the secondary ESS, the NaS battery has a high charge/discharge efficiency (85+%) [33]. Therefore, the charge and the discharge efficiency are both set as 93% with a round-trip efficiency of 86.5%. Being the secondary ESS, the energy capacity of the battery system is smaller since it is designed to adjust mismatches between the forecasted and the actual wind power. The total energy capacity is set as 2 h of the average wind power mismatches (a forecasting error of 10.78% in this study), which is 18 MWh. The limits for the state of charge are defined between 20% and 80% of the energy capacity, and the maximum charge and discharge powers are both defined as 2 MW. The LMP threshold $(LMP_{\rm thr})$ is set as the 75 percentile of the forecasting results to avoid unnecessary cycling.

B. Case Studies

As discussed in Section II-B, the accuracy of LMP forecasting becomes worse when price spikes happen. The dispatch strategy of two typical summer days, July 24 (without LMP spikes) and July 25 (with LMP spike), are used as examples to calculate the financial revenues, respectively.

To solve the optimization problem, CVX, a package for specifying and solving convex programs, is used [34], [35]. The dispatch results of the wind farm and ESS for July 24, when no LMP spikes happen, are shown in Figs. 5–8. In Fig. 5, the total forecasted wind power and the scheduled deliverable wind power are plotted to the left Y-axis. The LMP are plotted to the right Y-axis. A large portion of the wind power generated between 5 A.M. and 9 A.M. when the LMP is low (shown in Fig. 5) is shifted to the peak hours between 3 P.M. to 6 P.M. as shown by the solid curve which represents the total scheduled wind power

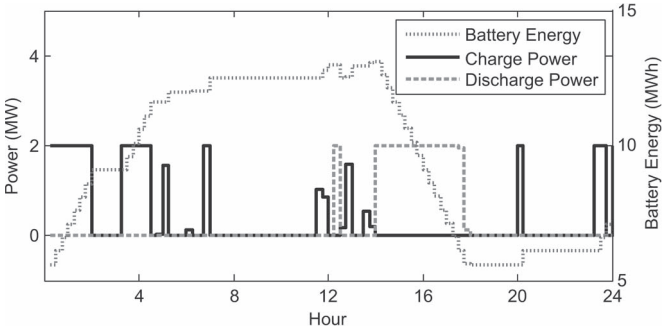

Fig. 7. Battery charge and discharge power (left axis) and battery energy (right axis) for July 24.

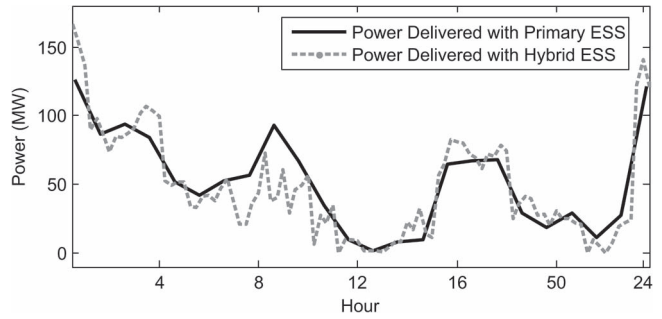

Fig. 8. Scheduled power delivered with primary ESS and actual power delivered to the grid with hybrid ESS for July 24.

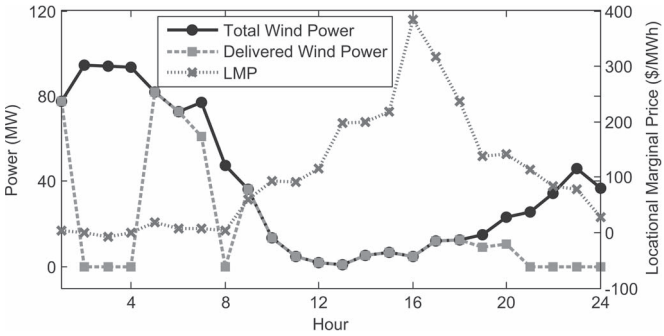

Fig. 9. Total wind power, delivered wind power (left axis), and LMP (with price spikes, right axis) for July 25.

in Fig. 8. The charge and discharge processes of both the primary ESS and secondary ESS are plotted in Figs. 6 and 7. The total actual output of the wind-storage system is plotted by the dashed line in Fig. 8. The total revenue of this case is \$45 832, while the original revenue without optimization is \$39 898.

The dispatch results for July 25, when LMP spikes happen, are shown in Figs. 9–12.

When comparing the dispatch results with the nonspike case, it can be observed that, when there are LMP spikes, more wind power is stored into ESS and discharged when the price is considered high and less wind power are directly delivered to the grid, as shown in Fig. 9. To take advantage of the tremendous LMP variations, both primary ESS and secondary ESS are cycled more often than the operation day without LMP spikes, as shown in Figs. 10 and 11. The total actual output of the wind-storage system is plotted by the dashed line in Fig. 12. The total revenue of this case is \$61 085, while the original revenue without optimal scheduling is \$30 761.

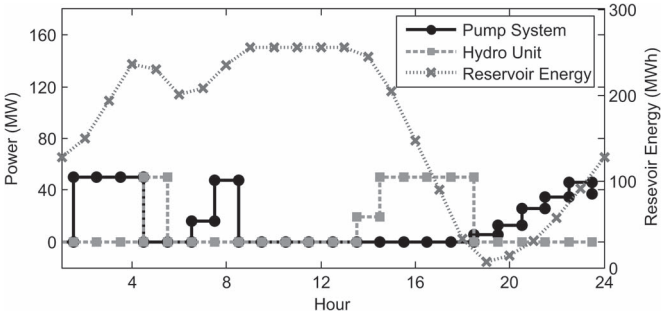

Fig. 10. Pump system consumption, hydro unit output (left axis), and water reservoir energy level (right axis) for July 25.

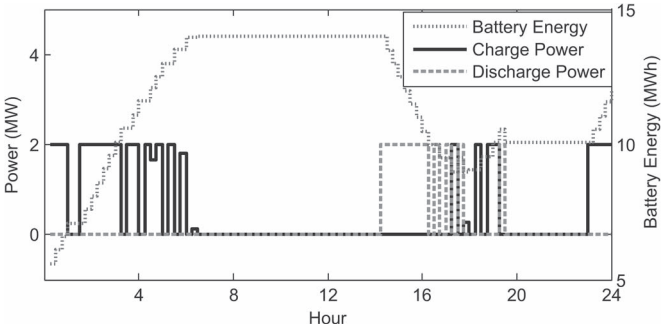

Fig. 11. Battery charge and discharge power (left axis) and battery energy (right axis) for July 25.

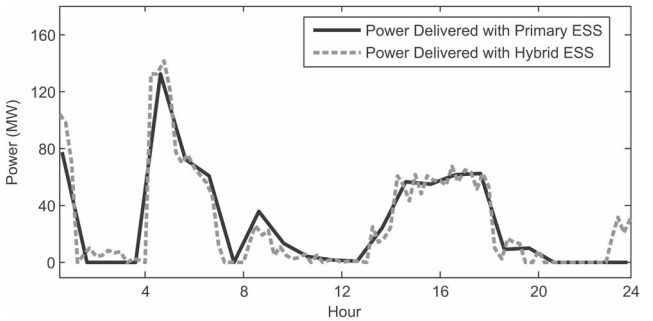

Fig. 12. Scheduled power delivered with primary ESS and actual power delivered to the grid with hybrid ESS for July 25.

TABLE I
DISPATCH AND ORIGINAL REVENUE COMPARISON

Date	Original Revenue (\$)	Dispatch Revenue (\$)	Increase (%)
July 24th (no LMP spikes)	39898	45925	15.11
July 25th (LMP spikes)	30761	61059	98.49

The dispatch results are compared and summarized in Table I. With hybrid ESS, the total revenue of the wind farm has satisfactory improvement for both operation days with and without LMP spikes. The revenue increase for July 24 is about 15.11%; the revenue increase for July 25 when the price cap goes up to \$400/MWh reaches 98.49%. Therefore, with accurately forecasted wind power and LMP information, the dispatch of the wind farm with the hybrid ESS system works as a profitable strategy in the deregulated electricity market.

VII. Conclusion

In this paper, the dispatch strategy for a wind farm with hybrid ESS is developed based on day-ahead wind power and LMP forecasting information. In general, the outputs of the wind generation resources are based upon wind conditions, and they participate in the electricity market as a price taker. While the potential benefits of large-scale ESS are recognized nowadays, some states have passed regulations about energy storage installation requirements. In this paper, a hybrid ESS with primary and secondary ESSs is designed to dispatch the total output of the wind-storage system according to LMP signals. The primary ESS is designed to optimize the system revenue according to day-ahead wind power and LMP forecasting, while the secondary ESS is applied to adjust the mismatches between actual values and forecasted values in real-time operation. Two cases studies for two typical summer operation days, one with LMP spikes and one without LMP spikes, are included to show the potential financial benefits of the dispatch strategy. The calculation results show that large financial benefits can be achieved by the proposed dispatch strategy, particularly for days with LMP spike days.

References

[1] Market Strategy Board (MSB), "Grid integration of large-capacity renewable energy sources and use of large-capacity electrical energy storage," IEC, Geneva, Switzerland, Oct. 2012.

[2] E. D. Castronuovo and J. A. P. Lopes, "Optimal operation and hydro storage sizing of a wind-hydro power plant," *Int. J. Elect. Power Energy Syst.*, vol. 26, no. 10, pp. 771–778, Dec. 2004.

[3] G. Giebel *et al.*, "The state of the art in short-term prediction of wind power—A literature overview," RisøDTU, Wind Energy Div., Roskilde, Denmark, Anemos Rep. v.1.1, 2003.

[4] S. Fan, J. R. Liao, R. Yokoyama, L. Chen, and W.-J. Lee, "Forecasting the wind generation using a two-stage network based on meteorological information," *IEEE Trans. Energy Convers.*, vol. 24, no. 2, pp. 474–482, Jun. 2009.

[5] A. Khosravi, S. Nahavandi, and D. Creighton, "Prediction intervals for short-term wind farm power generation forecasts," *IEEE Trans. Sustain. Energy*, vol. 4, no. 3, pp. 602–610, Jul. 2013.

[6] M. Lange and U. Focken, *Physical Approach to Short-Term Wind Power Prediction*. London, U.K.: Springer-Verlag, 2006.

[7] A. Kusiak and Z. Zijun, "Short-horizon prediction of wind power: A data-driven approach," *IEEE Trans. Energy Convers.*, vol. 25, no. 4, pp. 1112–1122, Dec. 2010.

[8] J. W. Taylor, P. E. McSharry, and R. Buizza, "Wind power density forecasting using ensemble predictions and time series models," *IEEE Trans. Energy Convers.*, vol. 24, no. 3, pp. 775–782, Sep. 2009.

[9] K. Methaprayoon, C. Yingvivatanapong, W.-J. Lee, and J. R. Liao, "An integration of ANN wind power estimation into unit commitment considering the forecasting uncertainty," *IEEE Trans. Ind. Appl.*, vol. 43, no. 6, pp. 1441–1448, Nov./Dec. 2007.

[10] J. L. Torres, A. García, M. De Blas, and A. De Francisco, "Forecast of hourly average wind speed with ARMA models in Navarre (Spain)," *Sol. Energy*, vol. 79, no. 1, pp. 65–77, Jul. 2005.

[11] R. G. Kavasseri and K. Seetharaman, "Day-ahead wind speed forecasting using f-ARIMA models," *Renew. Energy*, vol. 34, no. 5, pp. 1388–1393, May 2009.

[12] K. Bhaskar and S. N. Singh, "AWNN-assisted wind power forecasting using feed-forward neural network," *IEEE Trans. Sustain. Energy*, vol. 3, no. 2, pp. 306–315, Apr. 2012.

[13] P. Zhao *et al.*, "Performance evaluation and accuracy enhancement of a day-ahead wind power forecasting system in China," *Renew. Energy*, vol. 43, pp. 234–241, Jul. 2012.

[14] M. A. Mohandes, T. O/ Halawani, S. Rehman, and A. A. Hussain, "Support vector machines for wind speed prediction," *Renew. Energy*, vol. 29, no. 6, pp. 939–947, May 2004.

[15] D. Liu, D. Niu, H. Wang, and L. Fan, "Short-term wind speed forecasting using wavelet transform and support vector machines optimized by genetic algorithm," *Renew. Energy*, vol. 62, pp. 592–597, Feb. 2014.

[16] J. P. S. Catala, H. M. I. Pousinho, and V. M. F. Mendes, "Hybrid intelligent approach for short-term wind power forecasting in Portugal," *IET Renew. Power Gen.*, vol. 5, no. 3, pp. 251–257, May 2011.

[17] I. G. Damousis, M. C. Alexiadis, J. B. Theocharis, and P. S. Dokopoulos, "A fuzzy model for wind speed prediction and power generation in wind parks using spatial correlation," *IEEE Trans. Energy Convers.*, vol. 19, no. 2, pp. 352–361, Jun. 2004.

[18] M. Shahidehpour, H. Yamin, and Z. Li, *Market Operations in Electric Power Systems: Forecasting, Scheduling, Risk Management*. New York, NY, USA: Wiley-IEEE Press, 2002.

[19] J. P. S. Catalão, *Electric Power Systems: Advanced Forecasting Techniques and Optimal Generation Scheduling*. Boca Raton, FL, USA: CRC Press, 2012.

[20] P. Mandal, T. Senjyu, N. Urasaki, T. Funabashi, and A. K. Srivastava, "A novel approach to forecast electricity price for PJM using neural network and similar days method," *IEEE Trans. Power Syst.*, vol. 22, no. 4, pp. 2058–2065, Nov. 2007.

[21] N. M. Pindoriya, S. N. Singh, and S. K. Singh, "An adaptive wavelet neural network-based energy price forecasting in electricity markets," *IEEE Trans. Power Syst.*, vol. 23, no. 3, pp. 1423–1432, Aug. 2008.

[22] Y. Y. Hong and C. Y. Hsiao, "Locational marginal price forecasting in deregulated electricity markets using artificial intelligence," *Proc. Inst. Elect. Eng.—Gen. Transmiss. Distrib.*, vol. 149, no. 5, pp. 621–626, Sep. 2002.

[23] Z. Ning *et al.*, "Planning pumped storage capacity for wind power integration," *IEEE Trans. Sustain. Energy*, vol. 4, no. 2, pp. 393–401, Apr. 2013.

[24] S. O. Haykin, *Neural Networks and Learning Machines*, 3rd ed. Upper Saddle River, NJ, USA: Prentice-Hall, 2008.

[25] J. P. S. Catalão, H. M. I. Pousinho, and V. M. F. Mendes, "Short-term wind power forecasting in Portugal by neural networks and wavelet transform," *Renew. Energy*, vol. 36, no. 4, pp. 1245–1251, Apr. 2011.

[26] *Weather Underground*. [Online]. Available: http://www.wunderground.com/

[27] D. Phillips, "Nodal pricing basics," Jan. 2004. [Online]. Available: http://www.ieso.ca/Documents/consult/mep/LMP_NodalBasics_2004jan14.pdf

[28] *ERCOT 101 for Wind Generation Course Materials*, ERCOT, Austin, TX, USA, 2010.

[29] ERCOT Nodal Protocols. Section 6: Adjustment Period and Real-Time Operations, ERCOT, Austin, TX, USA, Oct. 1, 2014.

[30] H. Chen *et al.*, "Progress in electrical energy storage system: A critical review," *Progr. Nat. Sci.*, vol. 19, no. 3, pp. 291–312, Mar. 2009.

[31] T. Muche, "Optimal operation and forecasting policy for pump storage plants in day-ahead markets," *Appl. Energy*, vol. 113, pp. 1089–1099, Jan. 2014.

[32] CPUC, *Decision Adopting Energy Storage Procurement Framework and Design Program*, San Francisco, CA, USA, 2013. [Online]. Available: http://www.cpuc.ca.gov/PUC/energy/electric/storage.htm

[33] T. Oshima, M. Kajita, and A. Okuno, "Development of sodium-sulfur batteries," *Int. J. Appl. Ceram. Technol.*, vol. 1, no. 3, pp. 269–276, Jul. 2004.

[34] M. Grant and S. Boyd, "Graph implementations for nonsmooth convex programs," in *Recent Advances in Learning and Control (a Tribute to M. Vidyasagar)*, V. Blondel, S. P. Boyd, and H. Kimura, Eds. London, U.K.: Springer-Verlag, 2008, pp. 95–110.

[35] M. Grant and S. Boyd, CVX: Matlab Software for Disciplined Convex Programming Version 2.0 Beta, Sep. 2013. [Online]. Available: http://cvxr.com/cvx

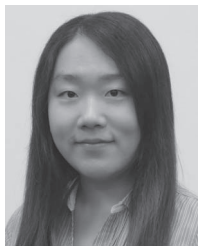

Meng Liu (S'12) received the B.S. degree from Shandong University, Jinan, China, in 2010. She is currently working toward the Ph.D. degree in energy systems at The University of Texas at Arlington, Arlington, TX, USA, where she is a member of the Energy Systems Research Center.

Her areas of research interest are renewable energy, energy storage, and energy storage integration to the smart grid.

Franklin L. Quilumba (S'10–M'14) received the Diploma degree in electrical engineering from the National Polytechnic School (Escuela Politecnica Nacional), Quito, Ecuador, in 2008, and the M.S. and Ph.D. degrees in electrical engineering from The University of Texas at Arlington (UTA), Arlington, TX, USA, in 2014.

He was a Postdoctoral Research Associate with the Energy Systems Research Center at UTA. In 2014, he joined the faculty of the National Polytechnic School, where he currently holds the title of Assistant Professor. His areas of research interest are power system analysis, operation, stability, and control; computer simulation of electric power systems; power load modeling; generation and transmission planning; demand response; and load forecasting.

Wei-Jen Lee (S'85–M'85–SM'97–F'07) received the B.S. and M.S. degrees from National Taiwan University, Taipei, Taiwan, in 1978 and 1980, respectively, and the Ph.D. degree from The University of Texas at Arlington, Arlington, TX, USA, in 1985, all in electrical engineering.

In 1985, he joined The University of Texas at Arlington, where he is currently a Professor in the Electrical Engineering Department and the Director of the Energy Systems Research Center. He has been involved in research on power flow, transient and dynamic stability, voltage stability, short circuits, relay coordination, power quality analysis, renewable energy, and deregulation for utility companies.

Prof. Lee is a Registered Professional Engineer in the State of Texas.